RESEARCH ARTICLE

Knockdown of UHRF1 by Lentivirus-mediated shRNA Inhibits Ovarian Cancer Cell Growth

Feng Yan[1,2], Li-Jia Shao[2], Xiao-Ya Hu[1]*

Abstract

Human UHRF1 (ubiquitin-like PHD and RING finger domain-containing 1) has been reported to be over-expressed in many cancers, but its role in ovarian cancer remains elusive. Here, we determined whether knockdown of UHRF1 by lentivirus-mediated shRNA could inhibit ovarian cancer cell growth. Lentivirus-mediated short hairpin RNAs (lv-shRNAs-UHRF1) were designed to trigger the gene silencing RNA interference (RNAi) pathway. The efficiency of lentivirus-mediated shRNA infection into HO-8910 and HO-8910 PM cells was determined using fluorescence microscopy to observe lentivirus-mediated GFP expressionand was confirmed to be over 80 percent. UHRF1 expression in infected HO-8910 and HO-8910 PM was evaluated by real-time PCR and Western blot analysis. The Cell Counting Kit-8 (CCK-8) assay was used to measure cell viability; flow cytometry and Hoechst 33342 assay was applied to measure cell cycle arrest and apoptosis. Cell invasion was assessed using transwell chambers. Our results demonstrated that the loss of UHRF1 promoted HO-8910 and HO-8910 PM cell apoptosis, while inhibiting cell proliferation. In addition, UHRF1 knockdown significantly inhibited the invasion of human ovarian cancer cells. In the present study, we also showed that depleting HO-8910 cells of UHRF1 caused activation of the DNA damage response pathway, with the cell cycle arrested in G2/M-phase. The DNA damage response in cells depleted of UHRF1 was illustrated by phosphorylation of CHK (checkpoint kinase) 2 on Thr68, phosphorylation of CDC25 (cell division control 25) on Ser 216 and phosphorylation of CDK1 (cyclin-dependent kinase 1) on Tyr 15.

Keywords: Ovarian cancer cells - UHRF1 - apoptosis - cell cycle - phosphorylation - transcription factors

Asian Pac J Cancer Prev, **16 (4)**, 1343-1348

Introduction

Cancer has been viewed as a set of diseases that are driven by wide-spread aberrant epigenetic changes that include mutations in tumour-suppressor genes and oncogenes, and chromosomal abnormalities. Ubiquitin-like with PHD and ring finger domains 1 (UHRF1) is a novel anti-apoptotic gene, and over-expression of UHRF1 is involved in tumorigenicity (Geng et al., 2012; Wang et al., 2012; Yang et al., 2012). UHRF1 also known as ICBP90 (inverted CCAAT box binding protein 90) identified as a multidomain protein is a nuclear protein that acts as a fundamental regulator in cell proliferation and maintains DNA methylation after replication and heterochromatin formation (Fang et al., 2012). UHRF1 contributes to silencing of tumor suppressor genes by recruiting DNA methyltransferase 1 (DNMT1) to their hemi-methylated promoters via its SRA domain and represses the expression of several tumour suppressor genes (TSGs) including p16INK4A, hMLH1, BRCA1, RB1 and E2F-1(Mousli et al., 2003). Conversely, UHRF1 is regulated by other TSGs such as p53, p73, p21Cip1/WAF1 (Arima et al., 2004; Alhosin et al., 2011; Achour et al., 2013).

In non-cancerous cells, UHRF1 is required for cell cycle progression. UHRF1 mRNA and protein fluctuate with the cell cycle (Tien et al., 2011). In cancer cells, UHRF1 levels are high and the protein is equally expressed in all phases of the cell cycle (Arima et al., 2004). For example, cancer cell lines such as HeLa, Jurkat and A549 show constant ICBP90 expression throughout the entire cell cycle (Mousli et al., 2003). However, reports on the effects of UHRF1 depletion in cancer cells have been varied. For example, Wang et al. found lentiviral-mediated RNA interference (RNAi) of UHRF1 induced apoptosis and cell cycle arrest at the G0/G1 phase in in colorectal cancer cell lines (Wang et al., 2012), but Dandache et al. and Tien et al. both assumed that a down-regulation of UHRF1, cell cycle arrest in G2/M-phase in different human colorectal cancer cell lines (Tien et al., 2011; Dandache et al., 2012). Arima et al. showed that HeLa cells remain blocked G1/S transition after DNA damage (Arima et al., 2004). Abbady et al. proposed that ICBP90 down-regulation is a key event in G1 arrest

*[1]College of Chemistry and Chemical Engineering, Yangzhou University, Yangzhou, [2]Department of clinical Laboratory,Nanjing Medical University Cancer Hospital & Jiangsu Cancer Hospital, Nanjing, China *For correspondence: xyhu@yzu.edu.cn, yanfeng1895@163.com*

preceding T cell death (Abbady et al., 2005). Jenkins et al. reported H1299 cells a modest 2-fold knockdown of UHRF1 by shRNA (small-hairpin RNA) causes cells to arrest in either the G1-orG2/M-phases (Jenkins et al., 2005). These data establish the possibility that depleting cancer cells of UHRF1 may lead to cell death.

Ovarian cancer is the most lethal gynecological cancer. Although at least 70% of patients respond to platinum-based chemotherapy, the majority of patients eventually relapse. Ovarian cancer is the most lethal of all gynecologic neoplasms. Early-stage malignancy is frequently asymptomatic and difficult to detect and thus, by the time of diagnosis, most women have advanced disease. Most of these patients, although initially responsive, eventually develop and succumb to drug-resistant metastases. The success of typical postsurgical regimens, usually a platinum/taxane combination, is limited by primary tumors being intrinsically refractory to treatment and initially responsive tumors becoming refractory to treatment, due to the emergence of drug-resistant tumor cells.

In the present study, we successfully constructed the tumor-specific lentivirus-mediated shRNA targeting UHRF1 gene. The tumor-specific RNA interference system efficiently and specifically knocked down UHRF1 expression, induced the apoptosis and inhibited cell growth in ovarian cancer cells. We test cell cycle of UHRF1 knockdown cancer cells by flow cytometry, found cell cycle arrest at the G2/M phase. Moreover, we found loss of UHRF1 induces G2/M arrest might be relative with DNA damage and response pathway.

Materials and Methods

Cell culture

HO-8910 and HO-8910 PM ovarian cells, obtained from the cell bank of the Chinese Academy of Science in Shanghai, China, were cultured in RPMI-1640 with 10% fetal bovine serum (Gibco), 100 U/mL penicillin, 100 μg/mL streptomycin at 37°C under 5% CO_2, and 95% humidified air.

Construction of vectors and lentiviruses

The lentiviral expressing short hairpin RNA (shRNA) targeting the sequence of UHRF1 gene (TGAAATACTGGCCCGAGAA) and negative control (TTCTCCGAACGTGTCACGT) were purchased from Shanghai Genechem Co. Ltd. Correct insertions of shRNA cassettes were confirmed by restriction mapping and direct DNA sequencing. The shRNA-expressing lentiviral were transfacted into 293T cells together with the lentiviral helper plasmids to generate respective lentiviruses. Infectious lentiviruses were harvested 48 h post-transfection, centrifuged to remove cell debris, and then filtered through 0.45 μm cellulose acetate filters. Virus titer was determined by fluorescence-activated cell sorting analysis of GFP positive 293T cells and was approximately 1×10^9 transducing units (TU)/mL medium. The ability of the five lv-shRNA-UHRF1 vectors to knock down UHRF1 was investigated using qPCR.

qPCR

HO-8910 and HO-8910 PM cells were divided into 3 groups: UHRF1 knowdown cells (kd), negative control cells (nc), blank control (bl). 4 d post-infection, total RNA was extracted with TRIzol (Invitrogen, California, USA). Reverse transcription (RT) was performed using a Reverse Transcriptase Kit (Promega). GAPDH was used as an endogenous control. qPCR was performed in triplicate using SYBR Mastermix on a TP800 (TaKaRa, Japan). The qPCR cycling conditions were: pre-degenerate at 95°C for 15 s, followed by 40 cycles of denaturation at 95°C for 5 s, annealing at 55°C for 30 s and extension at 72°C for 30 s; a final extension of 65°C for 30 s. Values were normalized to the expression of the β-actin gene using the 2-ΔΔCt method. UHRF1, sense: 5'-CGTGGTCCAGATGAACTCC-3'; antisense: 5'-CACGTTGGCGTAGAGTTCC-3'; for GAPDH, sense: 5'-TGACTTCAACAGCGACACCCA-3'; antisense: 5'-CACCCTGTTGCTGTAGCCAAA-3'.

Protein preparation and western blot analysis

Total protein of each group cell was extracted using precooled RIPA lysis buffer. The protein concentration was determined by Nano-drop 2000 spectrophotometer. 50 μg protein sample of each group cell was separated by 10% sodium dodecyl sulfate-polyacrylamide gel electrophoresis and transferred to polyvinylidene difluoride (PVDF) membranes that were blocked with 5% bovine serum albumin for 2 hours. Afterward, the membranes were incubated overnight with primary antibodies at 4°C. After washing three times for 15 min with TBST at room temperature, membranes were incubated with secondary peroxidase-conjugated goat anti-mouse secondary antibodies for 2 hours at room temperature. Following extensive washing, the immunoreactivity was visualized by enhanced chemiluminescence (ECL kit, Pierce Biotechnology), and membranes were exposed to Kodak XAR-5 films (Sigma-Aldrich). The antibody used, the protein they have been raised against and the dilutions they were used at are listed in Table 1.

CCK-8 assay

Cells were plated in 96-well plates at a density of 5000 cells per well. Then, at 24 h, 48 h, 72 h, 96 h, 10 μL CCK-8 solution was added into the medium (Dojindo, Kumamoto, Janpan) for 2 h at 37°C. Absorbance of each well was quantified at 450 nm with an automated ELISA reader (Bio-Tech Instruments, Winooski, VT, USA).

Flow cytometric apoptosis assay and Hoechst 33342 assay

Approximately 1×10^5 cells/well were plated in triplicate in 6-well plates. After 2 d, cells were harvested and washed twice with PBS. Then, remove the PBS, cells were resuspended in 100 μL Annexin V/PI incubation buffer and incubated for 15 min at room temperature in the dark. Binding buffer (400 μL) was then added to each sample and flow cytometry was performed. The percentage of apoptotic cells was determined on a FACSCalibur flow cytometer (BD, New Iersey, USA). Annexin V-FITC (fluorescein isothiocyanate)/PI (propidiumiodide) analysis

Table 1. Antibody Used

Antibody	Catalogue number	Supplier	Dilution used
UHRF1	Ab57083	Abcam	1:500
β-actin	SC-1616	Santa Cruz Biotechnology	1:2000
Cyclin-D2	#2924	Cell signal technology	1:1000
Cyclin-E	HE-11	Santa Cruz Biotechnology	1:200
Cyclin-B1	SC-752	Santa Cruz Biotechnology	1:200
CDK1	#9112	Cell signal technology	1:1000
Phospho-CDK1 Tyr15	#9111	Cell signal technology	1:800
CHK2	#2662	Cell signal technology	1:800
Phospho-CHK2 Thr68	#2661	Cell signal technology	1:1000
CDC 25	#3652	Cell signal technology	1:100
Phospho-CDC25	#9258	Cell signal technology	1:1000

was performed according to the manufacturer's protocol (Annexin VAPC Apoptosis Detection Kit, eBioscience, USA).

HO-8910 and HO-8910 PM cells at logarithmic growth were seeded in 6-well plates by density of 5×10^5 cells/mL. 4 d after transfection, three group cell were washed twice with PBS, then incubated with 2 mmol/L Hoechst 33342 (Beyotime, Jiangsu, China) for 15 min in dark at room temperature. Cells after stain were viewed under a fluorescence microscope (Leica, German). The images were recorded on a computer with a digital camera attached to the microscope, and the images were processed by computer. The Hoechst reagent was taken up by the nuclei of the cells, and apoptotic cells exhibited a bright blue fluorescence.

Cell cycle analysis

Cells were plated in 6-well plates. Logarithmically growing cells were synchronized. 48 hours later, cells were harvested by trypsinisation, washed twice with ice-cold phosphate-buffered saline (PBS), and fixed with 70% ethanol at -20°C overnight. Subsequently, the cells were digested with RNaseA at 37°C for 20 min. Finally, 100 ul of propidium iodide (PI) solution (50 mg/L) was added to the cell suspension and cells were stained at room temperature for 10 min. The reaction products were measured using the FACSARIA flow cytometer (Becton Dickenson). The experiments were carried out in triplicate.

Cell invasion assay

The ability of HO-8910 and HO-8910 PM cells invasion was detected using Transwells (8 μm pore size, millipore). The transwells were put into the 24-well plates. First, 0.1 mL matrigel (50 mg/mL, BD Biosciences) was added onto the plate surface and incubated for 2 h at 4°C. Freshly trypsinized and washed cells were suspended in RPMI-1640. Then 100 μL of the cell suspension (5×10^5 cells) was added to the upper chamber of each insert that was coated with Matrigel. Next, 450 μL of RPMI-1640 containing 10% fetal bovine serum was added into the lower compartment, and the cells were allowed to invade for 24 h at 37°C in a 5% CO_2 humidified incubator. After incubation, the cells were fixed with 95% absolute alcohol and stained with crystal violet. Cells on the upper surface of the filter were removed with the cotton swab and the cells that had invaded into the bottom surface of the filter were counted and imaged under an inverted microscope

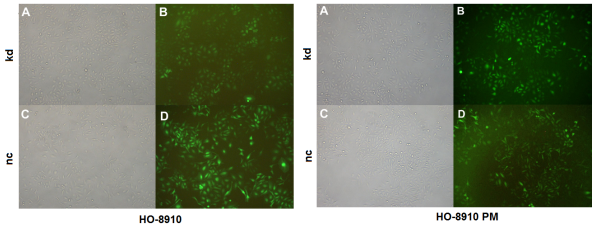

Figure 1. Efficient Infection with lv-shRNA-UHRF1 in HO-8910 and HO-8910 PM Cells. Pictures were taken at 72 hours after infection at a magnification of × 100. Decrease of UHRF1 mRNA and protein levels in human HO-8910 and HO-8910 PM cells

(Leica, German) at×200 magnification over ten random fields in each well. Each experiment was performed in triplicate.

Statistical analysis

Statistical analysis was performed with SPSS 16.0. Quantitative data were expressed as mean±standard deviation. Comparisons between multiple groups were conducted with one-way ANOVA, and those between two groups with SNK test. A value of $p<0.05$ was considered statistically significant.

Results

Lentivirus-mediated high-efficiency infection of HO-8910 and HO-8910 PM cells for knockdown of UHRF1

The concentration dose of lv-shRNAs-UHRF1 used was 1×10^9 TU/mL. The infection efficiency of HO-8910 and HO-8910 PM ovarian cancer cells was over 80 percent (Figure 1). The knockdown effect was analyzed by real-time PCR and Western blot analysis.

To determine the effect of lv-shRNA-UHRF1 on the expression of UHRF1 in HO-8910 and HO-8910 PM cells, mRNA and protein levels were analyzed. HO-8910 and HO-8910 PM cells were infected with either lv-shRNA-nc or lv-shRNA1-UHRF1. Four days post-infection, cells were collected and UHRF1 mRNA levels were detected by real-time PCR. Five days post-infection, cells were collected and protein levels were detected by Western blot analysis. As shown in Figure 2A, the infection of lv-shRNA-UHRF1 vectors resulted in a considerable decrease in the levels of UHRF1 mRNA compared with that of negative control group cells (nc) and blank (bl) group cells ($p<0.01$), while the expression was similar

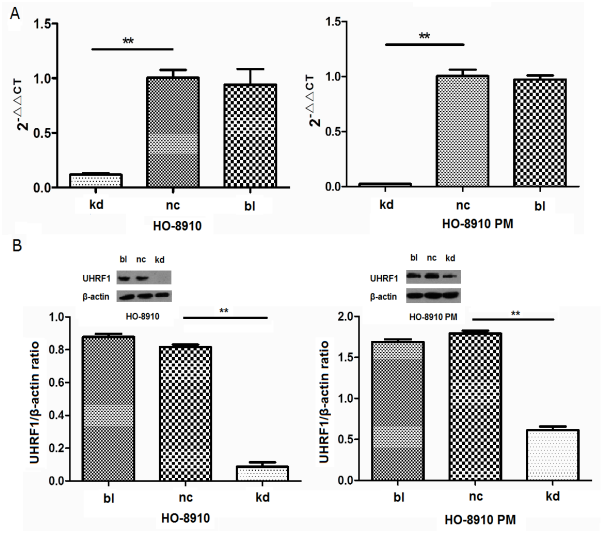

Figure 2. A) Decrease of UHRF1 mRNA Levels in HO-8910 and HO-8910 PM Cells Detected by Real-time PCR using the 2-ΔΔCt Method, and B) Knockdown of UHRF1 Protein Assayed by Western Blot Analysis. kd: UHRF1 Knockdown Cells; nc: Negative Control Cells; bl: blank control; β-actin: internal control protein. **P<0.01

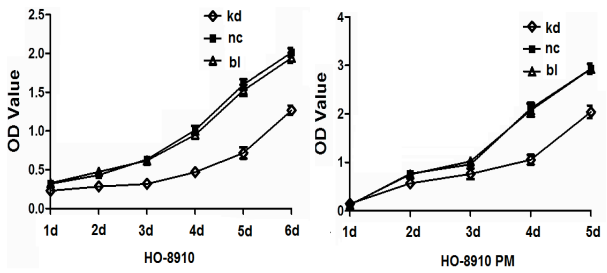

Figure 3. HO-8910 and HO-8910 PM Cell Growth Inhibition by Knockdown of UHRF1 with lv-shRNA-UHRF1 with CCK-8 Assay. HO-8910 and HO-8910 PM cell was both markedly reduced the proliferation potential since day 2 (p<0.01)

between nc group cells and bl group cells (p>0.05).

Western blot analysis demonstrated loss of UHRF1 protein expression in HO-8910 and HO-8910 PM cells treated with lv-shRNA-UHRF1 (p<0.01) (Figure 2B). The UHRF1 protein level was not affected in either bl group cells or the nc group cells (p>0.05). Therefore, lv-shRNA1-UHRF1 was used for the subsequent experiments in HO-8910 and HO-8910 PM cells.

Knockdown of UHRF1 noticeably inhibited HO-8910 and HO-8910 PM cells growth

To further evaluate the effect of UHRF1 on regulating ovarian cancer cell proliferation, CCK-8 assay was applied in both HO-8910 and HO-8910 PM cells. As shown in Figure 3, knockdown of UHRF1 expression markedly reduced the proliferation potential since day 2 (p<0.01).

Inhibition of UHRF1 increases cell death in HO-8910 and HO-8910 PM cells

To determine whether lv-shRNA-UHRF1 cause any apoptosis effects, flow cytometric apoptosis assay and Hoechst 33342 were applied. As shown in Figure 4A, lv-shRNA-UHRF1 did cause significant change in the profile

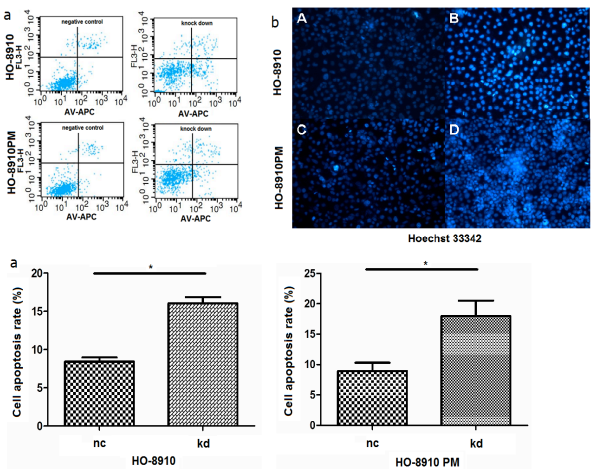

Figure 4. a) Apoptosis of Cells Infected with lv-shRNA-NC or lv-shRNA1-UHRF1 after Annexin-V-PI Staining, and b) Apoptotic Cells Including Early-stage (AV+/PI) and Late-stage (AV+/PI+) Apoptosis. A) HO-8910 negative control cells; **B)** HO-8910 UHRF1 knockdown cells; **C)** HO-8910 PM negative control cells; D) HO-8910 PM UHRF1 knockdown cells

of Annexin V-stained cell populations. The apoptosis rate of kd group cells was about 16%, and the nc group cells of that was about 8%. This result indicates that UHRF1 interferes with the progression of apoptosis in ovarian cancer cells. Hoechst 33342 was used to observe cell apoptosis more visible. The results were in accordance with flow cytometric apoptosis assay.

Cell invasion assay

The invasion activity of knockdown UHRF1 cells was estimated based on the number of cells that had migrated through the filter of the transwell chamber (Figure 5). The number of invased cells decreased in lv-shRNA-UHRF1 cells compared with the scrambled lv-shRNA-NC group cells.

Cell cycle analysis: UHRF1 depletion arrests cells in the G2/M-phase

To characterize the cell cycle behaviour of ovarian cancer cells depleted of UHRF1, we used flow cytometric apoptosis assay. As can be seen in Figure 6A, a small percentage of cells remain blocked in G2/M phase. The population of cells in HO-8910 in G2/M phase was increased from 2.5% to 4.2% after lv-shRNA-UHRF1 lentivirus infection (p<0.05). However, we never found any cell cycle arrest in HO-8910 PM cells.

Consistant with this, Western blot analysis did not show any change in the level of G1- or S-phase cyclins (Figure 6B), indicating that there was no cell cycle block in the G1- or S-phases. Instead, we saw an increase in the mitotic cyclin B1, suggesting that UHRF1 depletion caused a block after cyclin B systhesis.

Loss of UHRF1 associated with DNA damage pathway

Cyclin-dependent kinases are regulators of cell cycle progression. Because CDK1 (cyclin dependent kinase 1, also called Cdc2) is required for progression of cells from the G2-phase into and through mitosis, we questioned whether the G2/M-phase block was associated

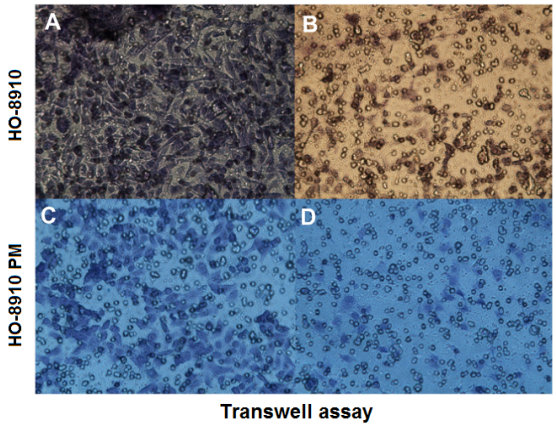

Figure 5. Invasion Activity of Knockdown UHRF1 Cells. A) HO-8910 negative control cells; **B)** HO-8910 UHRF1 knockdown cells; **C)** HO-8910 PM negative control assay; **D:)** HO-8910 PM UHRF1 knockdown cells

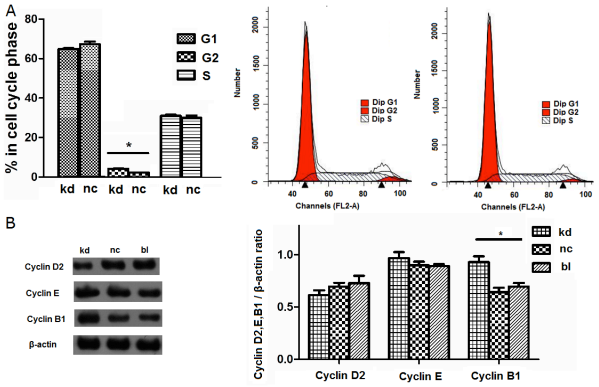

Figure 6. A) Percentage of HO-8910 Cells in the G1- , S- and G2/M-phase in kd, nc and bl Group Cells, and B) Levels of G1- and S-phase Cyclins D2 and E in UHRF1-depleted Cells and Cyclin B1 Level. β-Actin as a loading control for all experiments. *p<0.05.

with evidence of CDK1 inhibition. Figure 7 shows that phosphorylation of CDK1 on Tyr15 is enhanced in HO-8910 cells depleted of UHRF1, while total CDK1 remains constant (Figure 7).

The G2/M-phase checkpoint is activated as a response to DNA damage. For example, ultraviolet and ionizing irradiation or genotoxic drug treatment of cells causes cells to arrest in order to repair the damage. Because UHRF1 depletion renders cells more sensitive to DNA damaging agents, we hypothesized that the G2/M-phase block observed in UHRF1-depleted cells was associated with activation of the DNA damage pathway. To address this, we evaluated several markers of the DNA damage response in HO-8910 cells depleted of UHRF1. (i) CHK (checkpoint kinase) 2 is activated through phosphorylation by ATM and/or ATR kinase-mediated pathways in response to DNA damage. We find increased Thr68 phosphorylation of CHK2 in UHRF1-depleted cells. (ii) CDC25 (cell divison control 25) is the phosphatase responsible for removing the inhibitory

Discussion

Ovarian cancer is the most lethal gynecological cancer.

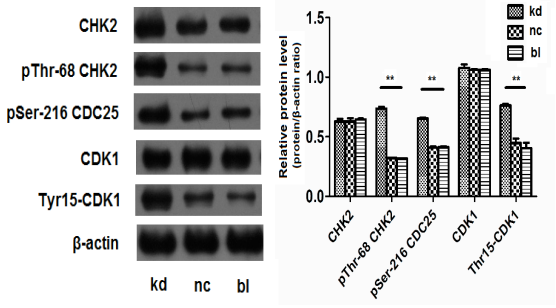

Figure 7. Markers of DNA Damage Pathway in UHRF1 Depletion Cells. Total CHK2 is unchanged (panel 1), but CHK2 is phosphorylated on Thr68 (panel 2) and CDC25 is phosphorylated on Ser216 (panel 3) are enhanced. Total cellular CDK1 (panel 4) is unchanged, but there are high level of Tyr15-phosphorylated CDK1 in UHRF1-deplated cells. **p<0.01

Survival rate of the cancer is still poor, partially because a large number of cancers are diagnosed at a late stage. Therefore, diagnostic markers of ovarian cancer are required to improve the current situation. UHRF1 had been reported over-expressed at high levels in many cancer cell lines and primary tumours, but its role in ovarian cancer remained elusive.

In this article, we researched the functional of UHRF1 in HO-8910 and HO-8910 PM ovarian cancer cells. We successfully constructed the tumor-specific lentivirus-mediated shRNA targeting UHRF1 gene and got UHRF1-depleted cell lines. In the UHRF1-depleted HO-8910 and HO-8910 PM cells, we found UHRF1 was associated with cancer cells growth. Knocked down UHRF1 expression would inhibited cell growth and induced cell apoptosis HO-8910 and HO-8910 PM cells. Further, we tested the cell cycle of UHRF1 knockdown cells by flow cytometry and found cell cycle arrest at the G2/M phase in HO-8910 cells. CDK1 is required for progression of cells from the G2-pahse into and through mitosis. We have found the evidence (Figure 7) that inhibitory phosphorylation of CDK1 on Tyr 15 is enhanced in HO-8910 cells depleted of UHRF1, while total CDK1 remains constant. However, we have not found cell cycle arrest in HO-8910 PM cells depleted of UHRF1. These data indicated that different cell lines depletion of UHRF1 caused cell cycle arrest different. Moreover, we evaluated several markers of the DNA damage response in HO-8910 cells depleted of UHRF1. We found increased Thr68 phosphorylation of CHK2 in UHRF1-depleted cells and increased phosphorylation of Ser 216 on CDC25 in cells depleted of UHRF1, confirming the downstream effect of CHK2 phosphorylation. These data demonstrate that the DNA damage response system is activated in response to UHRF1 depletion.

In summary, in the present study we provide evidence that UHRF1 play important role in ovarian cancer. Our result suggest that UHRF1 loss leads to cell death and cell-cylce block in ovarian cancer, which is associated with DNA damage pathway.

Acknowledgements

This work was financially supported by National Natural Science Foundation of China (21475063),

Jiangsu Provincial Special Program of Medical Science (BL2013036), Medicine Leading Talents of Jiangsu Health Department (LJ201131).

References

Abbady AQ, Bronner C, Bathami K, et al (2005). TCR pathway involves ICBP90 gene down-regulation via E2F binding sites. *Biochem Pharmacol*, **70**, 570-9.

Achour M, Mousli M, Alhosin M, et al (2013). Epigallocatechin-3-gallate up-regulates tumor suppressor gene expression via a reactive oxygen species-dependent down-regulation of UHRF1. *Biochem Biophys Res Commun*, **430**, 208-12.

Alhosin M, Sharif T, Mousli M, et al (2011). Down-regulation of UHRF1, associated with re-expression of tumor suppressor genes, is a common feature of natural compounds exhibiting anti-cancer properties. *J Exp Clin Cancer Res*, **30**, 41.

Arima Y, Hirota T, Bronner C, et al (2004). Down-regulation of nuclear protein ICBP90 by p53/p21Cip1/WAF1-dependent DNA-damage checkpoint signals contributes to cell cycle arrest at G1/S transition. *Genes to Cells*, **9**, 131-42.

Dandache I, et al (2012). Anti-cancer properties of cranberry juice in human colon cancer: Characterization of the cellular and molecular mechanisms. *Fundament Clin Pharmacol*, **26**, 40.

Fang L, Shanqu L, Ping G, et al (2012). Gene therapy with RNAi targeting UHRF1 driven by tumor-specific promoter inhibits tumor growth and enhances the sensitivity of chemotherapeutic drug in breast cancer *in vitro* and *in vivo*. *Cancer Chemotherapy Pharmacol*, **69**, 1079-87.

Geng Y, Gao Y, Ju H, et al (2012). Diagnostic and prognostic value of plasma and tissue ubiquitin-like, containing PHD and RING finger domains 1 in breast cancer patients. *Cancer Science*, **104**, 194-9.

Jenkins Y, Markovtsov V, Lang W, et al (2005). Critical role of the ubiquitin ligase activity of UHRF1, a nuclear RING finger protein, in tumor cell growth. *Molecular Biology of the Cell*, **16**, 5621-9.

Mousli M, Hopfner R, Abbady AQ, et al (2013). ICBP90 belongs to a new family of proteins with an expression that is deregulated in cancer cells. *Br J Cancer*, **89**, 120-7.

Tien AL, Senbanerjee S, Kulkarni A, et al (2011). UHRF1 depletion causes a G2/M arrest, activation of DNA damage response and apoptosis. *Biochemical J*, **435**, 175-85.

Wang F, Yang YZ, Shi CZ, et al (2012). UHRF1 promotes cell growth and metastasis through repression of p16 ink4a in colorectal cancer. *Ann Surgical Oncol*, **19**, 2753-62.

Yang G.L, Zhang LH, Bo JJ, et al (2012). UHRF1 is associated with tumor recurrence in non-muscle-invasive bladder cancer. *Medical Oncol*, **29**, 842-7.